



PUBLISHED FOR SISSA BY SPRINGER

RECEIVED: January 27, 2015

ACCEPTED: May 21, 2015

PUBLISHED: June 18, 2015

# Search for B decays to final states with the $\eta_c$ meson



## The BELLE collaboration

A. Vinokurova,<sup>d</sup> A. Kuzmin,<sup>d</sup> S. Eidelman,<sup>d</sup> A. Abdesselam,<sup>bc</sup> I. Adachi,<sup>n,j</sup>  
H. Aihara,<sup>bh</sup> K. Arinstein,<sup>d</sup> D.M. Asner,<sup>au</sup> T. Aushev,<sup>ak,v</sup> R. Ayad,<sup>bc</sup> A.M. Bakich,<sup>bb</sup>  
V. Bansal,<sup>au</sup> V. Bhardwaj,<sup>an</sup> B. Bhuyan,<sup>p</sup> A. Bobrov,<sup>d</sup> A. Bondar,<sup>d</sup> A. Bozek,<sup>aq</sup>  
M. Bračko,<sup>ag,w</sup> T.E. Browder,<sup>m</sup> V. Chekelian,<sup>ah</sup> B.G. Cheon,<sup>l</sup> K. Chilikin,<sup>v</sup>  
R. Chistov,<sup>v</sup> K. Cho,<sup>aa</sup> S.-K. Choi,<sup>k</sup> Y. Choi,<sup>ba</sup> D. Cinabro,<sup>bm</sup> J. Dingfelder,<sup>c</sup>  
Z. Doležal,<sup>e</sup> Z. Drásal,<sup>e</sup> A. Drutskoy,<sup>v,aj</sup> D. Dutta,<sup>p</sup> D. Epifanov,<sup>bh</sup> H. Farhat,<sup>bm</sup>  
J.E. Fast,<sup>au</sup> T. Ferber,<sup>g</sup> V. Gaur,<sup>bd</sup> N. Gabyshev,<sup>d</sup> A. Garmash,<sup>d</sup> R. Gillard,<sup>bm</sup>  
Y.M. Goh,<sup>l</sup> B. Golob,<sup>ae,w</sup> J. Haba,<sup>n,j</sup> K. Hayasaka,<sup>am</sup> H. Hayashii,<sup>an</sup> X.H. He,<sup>av</sup>  
W.-S. Hou,<sup>ap</sup> K. Inami,<sup>al</sup> A. Ishikawa,<sup>bg</sup> R. Itoh,<sup>n,j</sup> Y. Iwasaki,<sup>n</sup> D. Joffe,<sup>z</sup> T. Julius,<sup>ai</sup>  
K.H. Kang,<sup>ac</sup> E. Kato,<sup>bg</sup> C. Kiesling,<sup>ah</sup> D.Y. Kim,<sup>az</sup> H.J. Kim,<sup>ac</sup> J.H. Kim,<sup>aa</sup>  
K.T. Kim,<sup>ab</sup> M.J. Kim,<sup>ac</sup> S.H. Kim,<sup>l</sup> Y.J. Kim,<sup>aa</sup> K. Kinoshita,<sup>f</sup> B.R. Ko,<sup>ab</sup> P. Kodyš,<sup>e</sup>  
S. Korpar,<sup>ag,w</sup> P. Križan,<sup>ae,w</sup> P. Krokovny,<sup>d</sup> T. Kuhr,<sup>y</sup> T. Kumita,<sup>bj</sup> Y.-J. Kwon,<sup>bo</sup>  
J.S. Lange,<sup>h</sup> L. Li Gioi,<sup>ah</sup> J. Libby,<sup>q</sup> D. Liventsev,<sup>n</sup> P. Lukin,<sup>d</sup> D. Matvienko,<sup>d</sup>  
K. Miyabayashi,<sup>an</sup> H. Miyake,<sup>n,j</sup> H. Miyata,<sup>ar</sup> G.B. Mohanty,<sup>bd</sup> A. Moll,<sup>ah,be</sup> T. Mori,<sup>al</sup>  
R. Mussa,<sup>u</sup> E. Nakano,<sup>at</sup> M. Nakao,<sup>n,j</sup> Z. Natkaniec,<sup>aq</sup> C. Ng,<sup>bh</sup> N.K. Nisar,<sup>bd</sup>  
S. Nishida,<sup>n,j</sup> S. Ogawa,<sup>bf</sup> S. Okuno,<sup>x</sup> S.L. Olsen,<sup>ay</sup> P. Pakhlov,<sup>v,aj</sup> G. Pakhlova,<sup>v</sup>  
C.W. Park,<sup>ba</sup> H. Park,<sup>ac</sup> T.K. Pedlar,<sup>af</sup> R. Pestotnik,<sup>w</sup> M. Petrič,<sup>w</sup> L.E. Piilonen,<sup>bl</sup>  
E. Ribežl,<sup>w</sup> M. Ritter,<sup>ah</sup> A. Rostomyan,<sup>g</sup> Y. Sakai,<sup>n,j</sup> S. Sandilya,<sup>bd</sup> D. Santel,<sup>f</sup>  
L. Santelj,<sup>n</sup> T. Sanuki,<sup>bg</sup> Y. Sato,<sup>al</sup> V. Savinov,<sup>aw</sup> O. Schneider,<sup>ad</sup> G. Schnell,<sup>a,o</sup>  
C. Schwanda,<sup>t</sup> D. Semmler,<sup>h</sup> K. Senyo,<sup>bn</sup> O. Seon,<sup>al</sup> M.E. Sevier,<sup>ai</sup> V. Shebalin,<sup>d</sup>  
C.P. Shen,<sup>b</sup> T.-A. Shibata,<sup>bi</sup> J.-G. Shiu,<sup>ap</sup> B. Schwartz,<sup>d</sup> A. Sibidanov,<sup>bb</sup> F. Simon,<sup>ah,be</sup>  
Y.-S. Sohn,<sup>bo</sup> A. Sokolov,<sup>s</sup> E. Solovieva,<sup>v</sup> S. Stanič,<sup>as</sup> M. Starič,<sup>w</sup> M. Steder,<sup>g</sup>  
M. Sumihama,<sup>i</sup> T. Sumiyoshi,<sup>bj</sup> U. Tamponi,<sup>u,bk</sup> G. Tatishvili,<sup>au</sup> Y. Teramoto,<sup>at</sup>  
M. Uchida,<sup>bi</sup> T. Uglov,<sup>v,ak</sup> Y. Unno,<sup>l</sup> S. Uno,<sup>n,j</sup> C. Van Hulse,<sup>a</sup> P. Vanhoefer,<sup>ah</sup>  
G. Varner,<sup>m</sup> V. Vorobyev,<sup>d</sup> M.N. Wagner,<sup>h</sup> C.H. Wang,<sup>ao</sup> M.-Z. Wang,<sup>ap</sup> P. Wang,<sup>r</sup>  
Y. Watanabe,<sup>x</sup> K.M. Williams,<sup>bl</sup> E. Won,<sup>ab</sup> J. Yamaoka,<sup>au</sup> S. Yashchenko,<sup>g</sup> Y. Yook,<sup>bo</sup>  
Z.P. Zhang,<sup>ax</sup> V. Zhulanov,<sup>d</sup> and A. Zupanc<sup>w</sup>

- <sup>a</sup> *University of the Basque Country UPV/EHU, 48080 Bilbao, Spain*
- <sup>b</sup> *Beihang University, Beijing 100191, P.R. China*
- <sup>c</sup> *University of Bonn, 53115 Bonn, Germany*
- <sup>d</sup> *Budker Institute of Nuclear Physics SB RAS and Novosibirsk State University, Novosibirsk 630090, Russian Federation*
- <sup>e</sup> *Faculty of Mathematics and Physics, Charles University, 121 16 Prague, The Czech Republic*
- <sup>f</sup> *University of Cincinnati, Cincinnati, OH 45221, U.S.A.*
- <sup>g</sup> *Deutsches Elektronen-Synchrotron, 22607 Hamburg, Germany*
- <sup>h</sup> *Justus-Liebig-Universität Gießen, 35392 Gießen, Germany*
- <sup>i</sup> *Gifu University, Gifu 501-1193, Japan*
- <sup>j</sup> *The Graduate University for Advanced Studies, Hayama 240-0193, Japan*
- <sup>k</sup> *Gyeongsang National University, Chinju 660-701, South Korea*
- <sup>l</sup> *Hanyang University, Seoul 133-791, South Korea*
- <sup>m</sup> *University of Hawaii, Honolulu, HI 96822, U.S.A.*
- <sup>n</sup> *High Energy Accelerator Research Organization (KEK), Tsukuba 305-0801, Japan*
- <sup>o</sup> *IKERBASQUE, Basque Foundation for Science, 48013 Bilbao, Spain*
- <sup>p</sup> *Indian Institute of Technology Guwahati, Assam 781039, India*
- <sup>q</sup> *Indian Institute of Technology Madras, Chennai 600036, India*
- <sup>r</sup> *Institute of High Energy Physics, Chinese Academy of Sciences, Beijing 100049, P.R. China*
- <sup>s</sup> *Institute for High Energy Physics, Protvino 142281, Russian Federation*
- <sup>t</sup> *Institute of High Energy Physics, Vienna 1050, Austria*
- <sup>u</sup> *INFN - Sezione di Torino, 10125 Torino, Italy*
- <sup>v</sup> *Institute for Theoretical and Experimental Physics, Moscow 117218, Russian Federation*
- <sup>w</sup> *J. Stefan Institute, 1000 Ljubljana, Slovenia*
- <sup>x</sup> *Kanagawa University, Yokohama 221-8686, Japan*
- <sup>y</sup> *Institut für Experimentelle Kernphysik, Karlsruher Institut für Technologie, 76131 Karlsruhe, Germany*
- <sup>z</sup> *Kennesaw State University, Kennesaw GA 30144, U.S.A.*
- <sup>aa</sup> *Korea Institute of Science and Technology Information, Daejeon 305-806, South Korea*
- <sup>ab</sup> *Korea University, Seoul 136-713, South Korea*
- <sup>ac</sup> *Kyungpook National University, Daegu 702-701, South Korea*
- <sup>ad</sup> *École Polytechnique Fédérale de Lausanne (EPFL), Lausanne 1015, Switzerland*
- <sup>ae</sup> *Faculty of Mathematics and Physics, University of Ljubljana, 1000 Ljubljana, Slovenia*
- <sup>af</sup> *Luther College, Decorah, IA 52101, U.S.A.*
- <sup>ag</sup> *University of Maribor, 2000 Maribor, Slovenia*
- <sup>ah</sup> *Max-Planck-Institut für Physik, 80805 München, Germany*
- <sup>ai</sup> *School of Physics, University of Melbourne, Victoria 3010, Australia*
- <sup>aj</sup> *Moscow Physical Engineering Institute, Moscow 115409, Russian Federation*
- <sup>ak</sup> *Moscow Institute of Physics and Technology, Moscow Region 141700, Russian Federation*
- <sup>al</sup> *Graduate School of Science, Nagoya University, Nagoya 464-8602, Japan*
- <sup>am</sup> *Kobayashi-Maskawa Institute, Nagoya University, Nagoya 464-8602, Japan*
- <sup>an</sup> *Nara Women's University, Nara 630-8506, Japan*
- <sup>ao</sup> *National United University, Miao Li 36003, Taiwan*
- <sup>ap</sup> *Department of Physics, National Taiwan University, Taipei 10617, Taiwan*

- <sup>aq</sup> *H. Niewodniczanski Institute of Nuclear Physics, Krakow 31-342, Poland*  
<sup>ar</sup> *Niigata University, Niigata 950-2181, Japan*  
<sup>as</sup> *University of Nova Gorica, 5000 Nova Gorica, Slovenia*  
<sup>at</sup> *Osaka City University, Osaka 558-8585, Japan*  
<sup>au</sup> *Pacific Northwest National Laboratory, Richland, WA 99352, U.S.A.*  
<sup>av</sup> *Peking University, Beijing 100871, P.R. China*  
<sup>aw</sup> *University of Pittsburgh, Pittsburgh, PA 15260, U.S.A.*  
<sup>ax</sup> *University of Science and Technology of China, Hefei 230026, P.R. China*  
<sup>ay</sup> *Seoul National University, Seoul 151-742, South Korea*  
<sup>az</sup> *Soongsil University, Seoul 156-743, South Korea*  
<sup>ba</sup> *Sungkyunkwan University, Suwon 440-746, South Korea*  
<sup>bb</sup> *School of Physics, University of Sydney, NSW 2006, Australia*  
<sup>bc</sup> *Department of Physics, Faculty of Science, University of Tabuk, Tabuk 71451, Saudi Arabia*  
<sup>bd</sup> *Tata Institute of Fundamental Research, Mumbai 400005, India*  
<sup>be</sup> *Excellence Cluster Universe, Technische Universität München, 85748 Garching, Germany*  
<sup>bf</sup> *Toho University, Funabashi 274-8510, Japan*  
<sup>bg</sup> *Tohoku University, Sendai 980-8578, Japan*  
<sup>bh</sup> *Department of Physics, University of Tokyo, Tokyo 113-0033, Japan*  
<sup>bi</sup> *Tokyo Institute of Technology, Tokyo 152-8550, Japan*  
<sup>bj</sup> *Tokyo Metropolitan University, Tokyo 192-0397, Japan*  
<sup>bk</sup> *University of Torino, 10124 Torino, Italy*  
<sup>bl</sup> *CNP, Virginia Polytechnic Institute and State University, Blacksburg, VA 24061, U.S.A.*  
<sup>bm</sup> *Wayne State University, Detroit, MI 48202, U.S.A.*  
<sup>bn</sup> *Yamagata University, Yamagata 990-8560, Japan*  
<sup>bo</sup> *Yonsei University, Seoul 120-749, South Korea*

*E-mail:* [vinokurovanna@gmail.com](mailto:vinokurovanna@gmail.com)

**ABSTRACT:** We report a search for  $B$  decays to selected final states with the  $\eta_c$  meson:  $B^\pm \rightarrow K^\pm \eta_c \pi^+ \pi^-$ ,  $B^\pm \rightarrow K^\pm \eta_c \omega$ ,  $B^\pm \rightarrow K^\pm \eta_c \eta$  and  $B^\pm \rightarrow K^\pm \eta_c \pi^0$ . The analysis is based on  $772 \times 10^6$   $B\bar{B}$  pairs collected at the  $\Upsilon(4S)$  resonance with the Belle detector at the KEKB asymmetric-energy  $e^+e^-$  collider. We set 90% confidence level upper limits on the branching fractions of the studied  $B$  decay modes, independent of intermediate resonances, in the range  $(0.6\text{--}5.3) \times 10^{-4}$ . We also search for molecular-state candidates in the  $D^0 \bar{D}^{*0} - \bar{D}^0 D^{*0}$ ,  $D^0 \bar{D}^0 + \bar{D}^0 D^0$  and  $D^{*0} \bar{D}^{*0} + \bar{D}^{*0} D^{*0}$  combinations, neutral partners of the  $Z(3900)^\pm$  and  $Z(4020)^\pm$ , and a poorly understood state  $X(3915)$  as possible intermediate states in the decay chain, and set 90% confidence level upper limits on the product of branching fractions to the mentioned intermediate states and decay branching fractions of these states in the range  $(0.6\text{--}6.9) \times 10^{-5}$ .

**KEYWORDS:** Exotics, Quarkonium, e+-e- Experiments, B physics, Particle and resonance production

**ARXIV EPRINT:** [1501.06351](https://arxiv.org/abs/1501.06351)

---

## Contents

<b>1</b>	<b>Introduction</b>	<b>1</b>
<b>2</b>	<b>Event selection</b>	<b>2</b>
<b>3</b>	<b>Reconstruction of final states</b>	<b>4</b>
3.1	$B^\pm \rightarrow K^\pm \eta_c + \text{hadrons}$	4
3.2	$X_1(3872)$ , $X(3730)$ and $X(4014)$	6
3.3	$Z(3900)^0$ and $Z(4020)^0$	9
3.4	$X(3915)$	10
<b>4</b>	<b>Systematic uncertainties</b>	<b>11</b>
<b>5</b>	<b>Results</b>	<b>13</b>

---

## 1 Introduction

Many exotic charmonium-like states are observed in the mass region above the  $D\bar{D}$  threshold. Decays of  $B$  mesons provide a fruitful opportunity to study these states and to find new ones. For example, the state  $X(3872)$  was first observed by Belle in exclusive  $B^+ \rightarrow K^+ \pi^+ \pi^- J/\psi$  decays [1] that was later confirmed by CDF [2], DØ [3] and BaBar [4]. It was also observed in the LHCb experiment [5, 6] in  $pp$  collisions and  $B$  decays. The  $X(3872)$  mass is close to the  $m_{D^0} + m_{\bar{D}^{*0}}$  threshold, which engendered a hypothesis that this state may be a  $D^0 \bar{D}^{*0}$  molecule [7]. The observation of the decay  $X(3872) \rightarrow \gamma J/\psi$  by BaBar [8] and Belle [9] established the charged parity of  $X(3872)$  to be positive. Angular analysis of the  $X(3872) \rightarrow J/\psi \pi^+ \pi^-$  decay by LHCb [6] determined all its quantum numbers:  $J^{PC} = 1^{++}$ .

If  $X(3872)$  is indeed a  $D^0 \bar{D}^{*0}$  molecule, there can exist other “ $X(3872)$ -like” molecular states with different quantum numbers. Some may reveal themselves in the decays to final states containing the  $\eta_c$  meson. For example, a  $D^0 \bar{D}^{*0} - \bar{D}^0 D^{*0}$  combination (denoted hereinafter by  $X_1(3872)$ ) with quantum numbers  $J^{PC} = 1^{+-}$  would have a mass around  $3.872 \text{ GeV}/c^2$  and would decay to  $\eta_c \rho$  and  $\eta_c \omega$ . Combinations of  $D^0 \bar{D}^0 + \bar{D}^0 D^0$ , denoted by  $X(3730)$ , and  $D^{*0} \bar{D}^{*0} + \bar{D}^{*0} D^{*0}$ , denoted by  $X(4014)$ , with quantum numbers  $J^{PC} = 0^{++}$  would decay to  $\eta_c \eta$  and  $\eta_c \pi^0$ . The mass of the  $X(3730)$  state would be around  $2m_{D^0} = 3.730 \text{ GeV}/c^2$  while that of the  $X(4014)$  state would be near  $2m_{D^{*0}} = 4.014 \text{ GeV}/c^2$ .

Recently, a new charged state  $Z(3900)^\pm$  was found in  $Y(4260)$  decays by Belle [10] and BESIII [11]. Since this particle is observed in the decay to  $\pi^\pm J/\psi$ , it should contain at least four quarks. BESIII [12] reported subsequently an observation of another decay channel of the seemingly same state  $Z(3885)^\pm \rightarrow (D\bar{D}^*)^\pm$ . The  $Z(3900)^\pm$  was confirmed

in the decay to  $\pi^\pm J/\psi$  by an analysis of CLEO-c data [13] that also reported evidence for its neutral isotopic partner  $Z(3900)^0$ . Another exotic charged state  $Z(4020)^\pm$  was observed by BESIII in decays to  $\pi^\pm h_c$  [14] and  $(D^* \bar{D}^*)^\pm$  [15]. There are some indications from these analyses that the spin and parity of the charged states might be  $J^P = 1^+$ .

The near-threshold enhancement in the  $\omega J/\psi$  invariant mass distribution named  $Y(3940)$  was first observed by Belle in exclusive  $B \rightarrow K \omega J/\psi$  decays [16]. Later, in the same decay mode, BaBar discovered  $X(3915)$  [17], which was confirmed by Belle in two-photon production [18] and by other BaBar measurements [19, 20]. The parameters of  $Y(3940)$  are consistent with those of  $X(3915)$ , so they are considered to be the same particle. The quantum numbers of  $X(3915)$  are claimed to be  $J^{PC} = 0^{++}$ , but its nature is still undetermined, and there are several interpretations describing this state [21–25].

To search for the particles described above, we reconstruct  $\eta_c$  mesons via the  $K_S^0 K^\pm \pi^\mp$  mode and study the following four decays of charged  $B$  mesons:

1. the  $(\pi^+ \pi^-)$  decay mode:  $B^\pm \rightarrow K^\pm X \rightarrow K^\pm (\eta_c \pi^+ \pi^-)$ , where we look for  $X_1(3872)$ ,  $Z(3900)^0$  and  $Z(4020)^0$ ;
2. the  $(\omega)$  decay mode:  $B^\pm \rightarrow K^\pm X \rightarrow K^\pm (\eta_c \omega)$ , where we look for  $X_1(3872)$ ;
3. the  $(\eta)$  decay mode:  $B^\pm \rightarrow K^\pm X \rightarrow K^\pm (\eta_c \eta)$ , where we look for  $X(3730)$ ,  $X(4014)$  and  $X(3915)$ ;
4. the  $(\pi^0)$  decay mode:  $B^\pm \rightarrow K^\pm X \rightarrow K^\pm (\eta_c \pi^0)$ , where we look for  $X(3730)$ ,  $X(4014)$  and  $X(3915)$ .

## 2 Event selection

The analysis is based on a data sample that contains  $772 \times 10^6$   $B\bar{B}$  pairs, collected with the Belle detector at the KEKB asymmetric-energy  $e^+e^-$  collider [26],<sup>1</sup> [27]<sup>2</sup> operating at the  $\Upsilon(4S)$  resonance.

The Belle detector [28] (also see detector section in [29]) is a large-solid-angle magnetic spectrometer that consists of a silicon vertex detector, a 50-layer central drift chamber (CDC) for charged particle tracking and specific ionization measurement ( $dE/dx$ ), an array of aerogel threshold Cherenkov counters (ACC), time-of-flight scintillation counters (TOF), and an array of 8736 CsI(Tl) crystals for electromagnetic calorimetry located inside a superconducting solenoid coil that provides a 1.5 T magnetic field. An iron flux return yoke located outside the coil is instrumented to detect  $K_L^0$  mesons and identify muons. We use a GEANT3-based Monte Carlo (MC) simulation to model the response of the detector and determine its acceptance [30].

Charged tracks are selected with requirements based on the goodness of fit of the tracks and their impact parameters relative to the interaction point (IP). We require that the polar angle of each track be in the angular range ( $18^\circ$ – $152^\circ$ ) and that the track momentum perpendicular to the positron beamline be greater than 100 MeV/ $c$ .

<sup>1</sup>And other papers included in this volume.

<sup>2</sup>And following articles up to 03A011.

Pions and kaons are distinguished by combining the responses of the ACC and the TOF with  $dE/dx$  measurements in the CDC to form a likelihood ratio  $\mathcal{L}_{i/j} = \mathcal{L}_i/(\mathcal{L}_i + \mathcal{L}_j)$ . Here,  $\mathcal{L}_i$  is the likelihood that the particle is of type  $i$ .  $K_S^0$  candidates are reconstructed via the  $\pi^+\pi^-$  final state. The  $\pi^+\pi^-$  invariant mass must lie in the range  $0.486 \text{ GeV}/c^2 < M(\pi^+\pi^-) < 0.510 \text{ GeV}/c^2$ . The flight length of the  $K_S^0$  is required to lie within the interval  $(0.1 - 20) \text{ cm}$ . The angle  $\varphi$  between the pion pair momentum and the line joining the  $\pi^+\pi^-$  the vertex to the IP must satisfy  $\cos \varphi > 0.95$ .

The invariant masses of intermediate resonances must lie within ranges obtained from signal MC and containing more than 95% of the signal yield:  $2.9254 \text{ GeV}/c^2 < M(K_S^0 K^\pm \pi^\mp) < 3.0454 \text{ GeV}/c^2$  for the  $\eta_c$  meson,  $0.758 \text{ GeV}/c^2 < M(\pi^+\pi^-\pi^0) < 0.808 \text{ GeV}/c^2$  for the  $\omega$  meson,  $0.125 \text{ GeV}/c^2 < M(\gamma\gamma) < 0.145 \text{ GeV}/c^2$  for the  $\pi^0$  meson,  $0.528 \text{ GeV}/c^2 < M(\gamma\gamma) < 0.568 \text{ GeV}/c^2$  and  $0.538 \text{ GeV}/c^2 < M(\pi^+\pi^-\pi^0) < 0.558 \text{ GeV}/c^2$  for the  $\eta$  meson.

$B$  candidates are identified by their center-of-mass (c.m.) energy difference  $\Delta E = (\sum_i E_i) - E_b$ , and the beam-constrained mass  $M_{bc} = \sqrt{E_b^2/c^2 - (\sum_i \vec{p}_i)^2/c^2}$ , where  $E_b = \sqrt{s}/2$  is the beam energy in the  $\Upsilon(4S)$  c.m. frame, and  $\vec{p}_i$  and  $E_i$  are the c.m. three-momenta and energies, respectively, of the  $B$  candidate decay products. We define the signal region by  $|\Delta E| < 0.02 \text{ GeV}$  and  $5.273 \text{ GeV}/c^2 < M_{bc} < 5.285 \text{ GeV}/c^2$ ; the  $|\Delta E|$  range extends to  $0.04 \text{ GeV}$  for some decay channels.

Although the continuum background ( $e^+e^- \rightarrow q\bar{q}$ , where  $q = u, d, s, c$ ) is not dominant, we suppress it using topological criteria. Since the produced  $B$  mesons are nearly at rest in the c.m. frame, the signal tends to be isotropic, while the continuum  $q\bar{q}$  background tends to have a two-jet structure. We use the angle  $\Theta_{\text{thrust}}$  between the thrust axis<sup>3</sup> of the  $B$  candidate and that of the rest of the event to discriminate between these two cases. The distribution of  $|\cos \Theta_{\text{thrust}}|$  is strongly peaked near 1 for  $q\bar{q}$  events but nearly uniform for  $\Upsilon(4S) \rightarrow B\bar{B}$  events; we require  $|\cos \Theta_{\text{thrust}}| < 0.8$ . In addition, we require that the c.m. polar angle  $\theta_B$  of the reconstructed  $B$  meson satisfies  $|\cos \theta_B| < 0.8$ , where this angle is measured relative to the  $z$  axis that is collinear with the positron beam.

The mean number of multiple  $B$  candidates per event varies from 1.2 to 2.0, depending on the decay channel. If an event has multiple  $B$  candidates, we select the candidate with the minimum value of the following expressions in the order described below:

1.  $|m_{K_S^0} - M(\pi^+\pi^-)|$ ,
2.  $|m_{\eta_c} - M(K_S^0 K^\pm \pi^\mp)|$ ,
3.  $|m_\eta - M(\gamma\gamma)|$  (for  $\eta \rightarrow \gamma\gamma$  in the  $(\eta)$  mode) or  $|m_{\pi^0} - M(\gamma\gamma)|$  (for the  $(\omega)$  mode, for  $\eta \rightarrow \pi^+\pi^-\pi^0$  in the  $(\eta)$  mode and for the  $(\pi^0)$  mode),
4. maximum difference between  $z$  coordinates at the closest-distance point to the  $z$  axis among each pair of charged particles in the signal- $B$  final state.

According to MC, this procedure selects the correct  $B$  candidate with 95% probability.

<sup>3</sup>I.e., axis  $\hat{n}$  that maximizes  $\sum_i |\hat{p}_i \cdot \hat{n}|$ , where the sum is over all considered particles momenta  $\hat{p}_i$ .

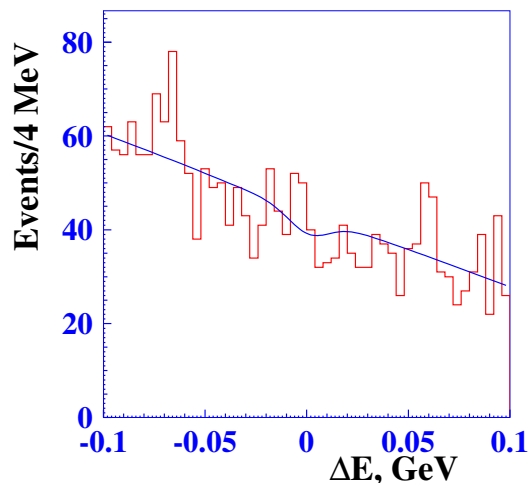


**Figure 1.** The  $\Delta E$  distribution for the decay  $B^\pm \rightarrow K^\pm \eta_c \omega$ .

### 3 Reconstruction of final states

#### 3.1 $B^\pm \rightarrow K^\pm \eta_c + \text{hadrons}$

We search for  $D^{(*)0} D^{(*)0}$  molecular-state candidates  $Z(3900)^0$ ,  $Z(4020)^0$ , and  $X(3915)$  in the following  $B$  meson decays:  $B^\pm \rightarrow K^\pm \eta_c \pi^+ \pi^-$ ,  $B^\pm \rightarrow K^\pm \eta_c \omega$ ,  $B^\pm \rightarrow K^\pm \eta_c \eta$ , and  $B^\pm \rightarrow K^\pm \eta_c \pi^0$ . To determine the branching fractions, we perform a binned maximum-likelihood fit of the  $\Delta E$  distribution that is modelled by a peaking signal and featureless background. For the  $(\pi^+ \pi^-)$ ,  $(\omega)$  and  $(\pi^0)$  decay modes, the signal function is the sum of two Gaussians ( $G$ ) and the background function is a linear polynomial; the fitting function is

$$f(x) = N_s [\alpha G(x_1, \sigma_1) + (1 - \alpha) G(x_2, \sigma_2)] + c_0 + c_1 x. \quad (3.1)$$

For a given mode, we generate signal MC and fix the mean values  $x_1$  and  $x_2$ , the standard deviations  $\sigma_1$  and  $\sigma_2$ , and the fraction of the first Gaussian  $\alpha$ ; we also obtain the detection efficiency for the mode. Here and in the following the detector resolution is taken into account. To account for the difference in resolution between MC and data, we replace the resolution of the dominant second Gaussian in the fit with  $\sigma'_2 = \sqrt{\sigma_2^2 + \delta^2}$ , where the resolution degradation  $\delta = (7.1 \pm 2.3) \text{ MeV}/c^2$  is taken from the analysis of the decay  $B^\pm \rightarrow K^\pm \eta_c (2S) \rightarrow K^\pm (K_S^0 K^\pm \pi^\mp)$  [31]. The  $\Delta E$  distribution for the  $(\omega)$  mode is shown in figure 1.

In the  $(\pi^+ \pi^-)$  and  $(\pi^0)$  modes, we observe some significant signal and so perform a two-dimensional fit of the  $K_S K \pi$  invariant mass ( $x$ ) and  $\Delta E$  ( $y$ ) distributions:

$$f(x, y) = N_s u(x) v(y) + N_{\text{non-res}} v(y) + c_0 + c_1 x + c_2 y, \quad (3.2)$$

$$u(x) = b(M_{\eta_c}, \Gamma_{\eta_c}) \otimes G(0, \sigma_{\text{res}}), \quad (3.3)$$

$$v(y) = \begin{cases} \alpha G(y_1, \sigma_1) + (1 - \alpha) G(y_2, \sigma_2) \\ G_{\text{LG}}(y_0, \sigma, P) \end{cases} \quad (3.4)$$

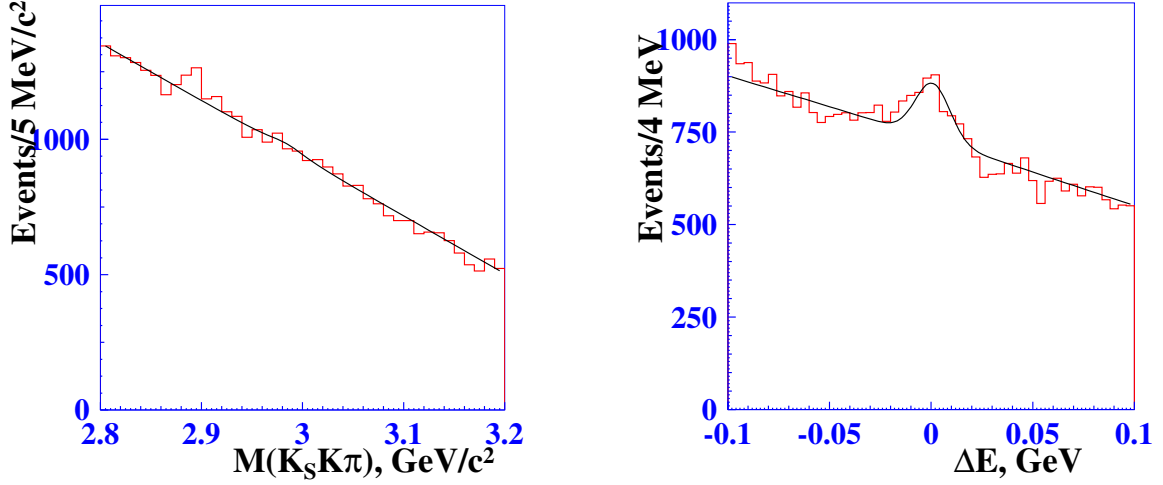


**Figure 2.** Projections of the two-dimensional fit in  $K_S K \pi$  invariant mass (left) and  $\Delta E$  (right) for the decay  $B^\pm \rightarrow K^\pm \eta_c \pi^+ \pi^-$ . Each projection is plotted for events in the whole fitting range of the other projection.

for the  $(\pi^+ \pi^-)$  and  $(\pi^0)$  modes, respectively. The logarithmic Gaussian function is defined as

$$G_{\text{LG}}(x_0, \sigma, P) = \frac{P}{\sqrt{2\pi}\sigma\sigma_0} e^{-\frac{\ln^2(1-P(x-x_0)/\sigma)}{2\sigma_0^2} - \frac{\sigma_0^2}{2}},$$

where  $\sigma_0 = \frac{1}{\sqrt{2\ln 2}} \sinh^{-1}(P\sqrt{2\ln 2})$  and  $P$  is the asymmetry parameter. The function  $u(x)$  characterizes the  $\eta_c$  resonance and is described by the convolution of a Breit-Wigner ( $b$ ) function and a Gaussian detector resolution function with  $\sigma_{\text{res}} = 6.2 \text{ MeV}/c^2$  obtained from ref. [31]. The parameter  $N_{\text{non-res}}$  represents the number of events that do not contain an intermediate  $\eta_c$  meson, but have the same final state. According to the fit, most of the events in the  $\Delta E$  peak are of that origin. The  $M(K_S K \pi)$  and  $\Delta E$  distributions for  $(\pi^+ \pi^-)$  and  $(\pi^0)$  modes are shown in figures 2 and 3, respectively.

To improve the  $\Delta E$  resolution in the  $(\eta)$  mode, we modify the energy of the  $\eta$  candidate decaying into photons:  $E'_\eta = c\sqrt{m_\eta^2 c^2 + p_\eta^2}$ , where  $m_\eta = 547.853 \text{ MeV}/c^2$  [33] is the mass and  $p_\eta$  is the reconstructed momentum. Since the  $\eta$  candidate is reconstructed in two decay modes, we perform a combined fit of the  $\Delta E$  distribution corresponding to  $\eta \rightarrow \gamma\gamma$  and  $\eta \rightarrow \pi^+ \pi^- \pi^0$ , using the following function:

$$f_i(x) = N_{\text{eff}} \varepsilon_i \mathcal{B}_i [\alpha_i G(x_{1,i}, \sigma_{1,i}) + (1 - \alpha_i) G(x_{2,i}, \sigma_{2,i})] + c_{0,i} + c_{1,i} x, \quad (3.5)$$

where  $i$  refers to either  $\eta \rightarrow \gamma\gamma$  or  $\eta \rightarrow \pi^+ \pi^- \pi^0$  decay. In particular,  $\mathcal{B}_{2\gamma} = \mathcal{B}(\eta \rightarrow \gamma\gamma)$  and  $\mathcal{B}_{3\pi} = \mathcal{B}(\eta \rightarrow \pi^+ \pi^- \pi^0) \times \mathcal{B}(\pi^0 \rightarrow \gamma\gamma)$ . Here, the parameter  $N_{\text{eff}}$  is the effective number of signal events. To obtain the total yield for each decay channel, it should be multiplied by the corresponding efficiency  $\varepsilon_{2\gamma/3\pi}$  and  $\eta$  decay branching fraction  $\mathcal{B}_i$ . The combined fit projections of the  $\Delta E$  distributions for the  $(\eta)$  mode are shown in figure 4.

The fit results are summarized in table 1.



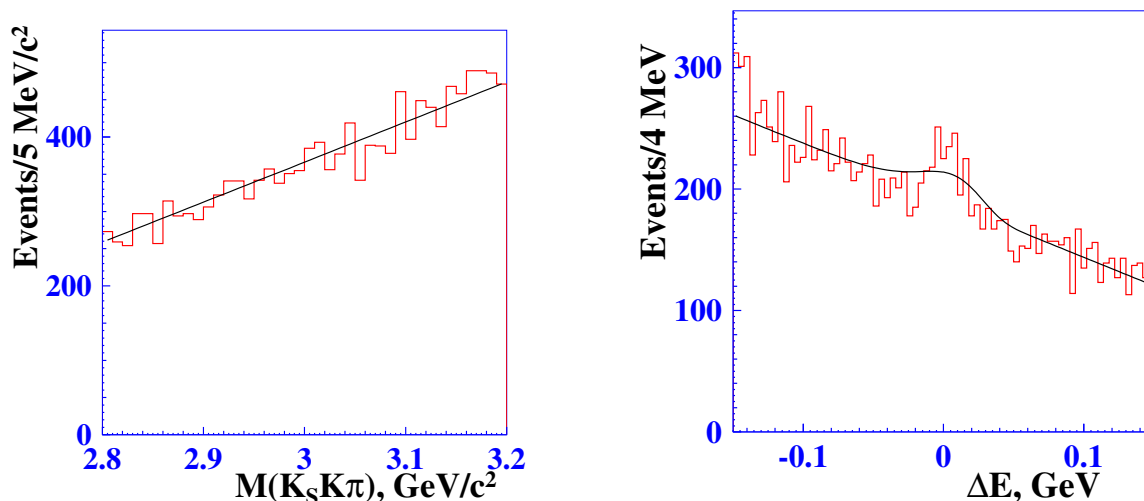


**Figure 3.** Projections of the two-dimensional fit in  $K_S K \pi$  invariant mass (left) and  $\Delta E$  (right) for the decay  $B^\pm \rightarrow K^\pm \eta_c \pi^0$ . Each projection is plotted for events in the whole fitting range of the other projection.

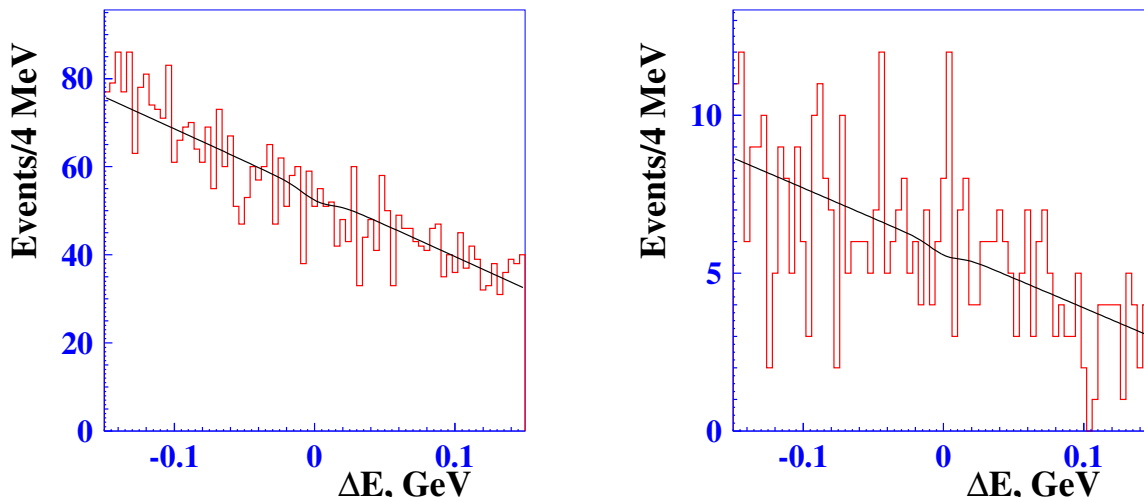


**Figure 4.** The combined fit projections of the  $\Delta E$  distributions in case of the  $\eta \rightarrow \gamma\gamma$  (left) and  $\eta \rightarrow \pi^+ \pi^- \pi^0$  (right) modes for the decay  $B^\pm \rightarrow K^\pm \eta_c \eta$ .

### 3.2 $X_1(3872)$ , $X(3730)$ and $X(4014)$

For the  $(\pi^+ \pi^-)$  mode, we perform a maximum-likelihood fit of the  $\eta_c \pi^+ \pi^-$  invariant mass distribution that is, again, modeled by a peaking signal and a smooth background; the fit function is

$$f(x) = N_s [\alpha G(M, \sigma_1) + (1 - \alpha) G(M, \sigma_2)] + c_0 + c_1 x. \quad (3.6)$$

For each intermediate resonance, we generate signal MC that incorporates the corresponding “ $X(3872)$ -like” particle quantum numbers. From the signal-MC fit, we fix the mean value  $M$ , the standard deviations  $\sigma_1$  and  $\sigma_2$ , and the Gaussian fraction  $\alpha$ ; in addition, we obtain the detection efficiency for the mode. From the fit, we obtain the signal yield

Decay mode	Fitting function	Efficiency, %	Yield
$B^\pm \rightarrow K^\pm \eta_c \omega$	(3.1)	$0.53 \pm 0.01$	$-41 \pm 27$
$B^\pm \rightarrow K^\pm \eta_c \pi^+ \pi^-$	(3.2) + (3.3) + (3.4)	$2.84 \pm 0.02$	$155 \pm 72$
$B^\pm \rightarrow K^\pm \eta_c \pi^0$		$3.69 \pm 0.01$	$-1.9 \pm 12.1$
$B^\pm \rightarrow K^\pm \eta_c \eta$ ,	(3.5)		
$\eta \rightarrow \gamma\gamma$		$3.05 \pm 0.01$	$-14 \pm 26$
$\eta \rightarrow \pi^+ \pi^- \pi^0$		$0.69 \pm 0.01$	$-1.8 \pm 3.4$

**Table 1.** Fit results for  $B$  decays independent of intermediate resonances.

$N_s$ , which is shown in table 2. The  $\eta_c \pi^+ \pi^-$  invariant mass distribution is shown in figure 5 (left).

We validate our procedure by applying it to the decay  $B^\pm \rightarrow K^\pm \psi(2S)$ ,  $\psi(2S) \rightarrow J/\psi \pi^+ \pi^-$ . This decay is similar to the  $(\pi^+ \pi^-)$  decay except that we reconstruct the  $\psi(2S)$  meson in place of the  $X_1(3872)$  and the  $J/\psi$  in place of the  $\eta_c$ . The  $J/\psi$  meson, like the  $\eta_c$ , is reconstructed via the  $K_S^0 K^\pm \pi^\mp$  final state. The selection criteria for this decay are the same as for the  $(\pi^+ \pi^-)$  decay except for the invariant mass of the  $K_S^0 K^\pm \pi^\mp$  combination:  $3.077 \text{ GeV}/c^2 < M(K_S^0 K^\pm \pi^\mp) < 3.117 \text{ GeV}/c^2$ . The mean number of  $B$  candidates per event is 1.7. In case of multiple  $B$  candidates, the one with the minimum differences for  $|m_{K_S^0} - M(\pi^+ \pi^-)|$  and  $|m_{J/\psi} - M(K_S^0 K^\pm \pi^\mp)|$  and the best vertex coordinate is chosen. We fit the  $J/\psi \pi^+ \pi^-$  invariant mass distribution and obtain the number of signal events  $N_s = 20.2 \pm 6.5$ , which corresponds to a significance of 3.5 standard deviations ( $\sigma$ ). The significance is estimated using the value of  $-2\sqrt{\ln \frac{\mathcal{L}_0}{\mathcal{L}_{\max}}}$ , where  $\mathcal{L}_{\max}$  ( $\mathcal{L}_0$ ) denotes the likelihood value when the yield is allowed to vary (is set to zero). The expected number of events estimated using the world averages of the known branching fractions [33] is  $22 \pm 4$ , which is consistent with  $N_s$ .

In the analysis of the  $(\omega)$  mode, we use the sum of two Gaussians to describe the signal and a threshold square-root function to describe the background:

$$f(x) = N_s [\alpha G(M, \sigma_1) + (1 - \alpha) G(M, \sigma_2)] + c_0 \sqrt{x - c_1}. \quad (3.7)$$

The  $\eta_c \omega$  invariant mass distribution is shown in figure 5 (right).

In the  $X(3730)$  mass region of the  $(\eta)$  mode, the fitting function is

$$f_i(x) = N_{\text{eff}} \varepsilon_i \mathcal{B}_i [\alpha_i G(M_i, \sigma_{1,i}) + (1 - \alpha_i) G(M_i, \sigma_{2,i})] + c_{0,i} + c_{1,i} x, \quad (3.8)$$

where  $N_{\text{eff}}$  is the effective number of signal events and  $i$  refers to either  $\eta \rightarrow \gamma\gamma$  or  $\eta \rightarrow \pi^+ \pi^- \pi^0$  decay. The  $\eta_c \eta$  invariant mass distributions in the  $X(3730)$  mass region are shown in figure 6 (top).

In the  $X(4014)$  mass region of the  $(\eta)$  mode, the fitting function is

$$f(x) = \begin{cases} N_{\text{eff}} \varepsilon_{2\gamma} \mathcal{B}_{2\gamma} G_{\text{LG}}(M_{2\gamma}, \sigma_{2\gamma}, P) + c_{0,1} + c_{1,1} x, \\ N_{\text{eff}} \varepsilon_{3\pi} \mathcal{B}_{3\pi} [\alpha G(M_{3\pi}, \sigma_{1,3\pi}) + (1 - \alpha) G(M_{3\pi}, \sigma_{2,3\pi})] + c_{0,2} + c_{1,2} x. \end{cases} \quad (3.9)$$

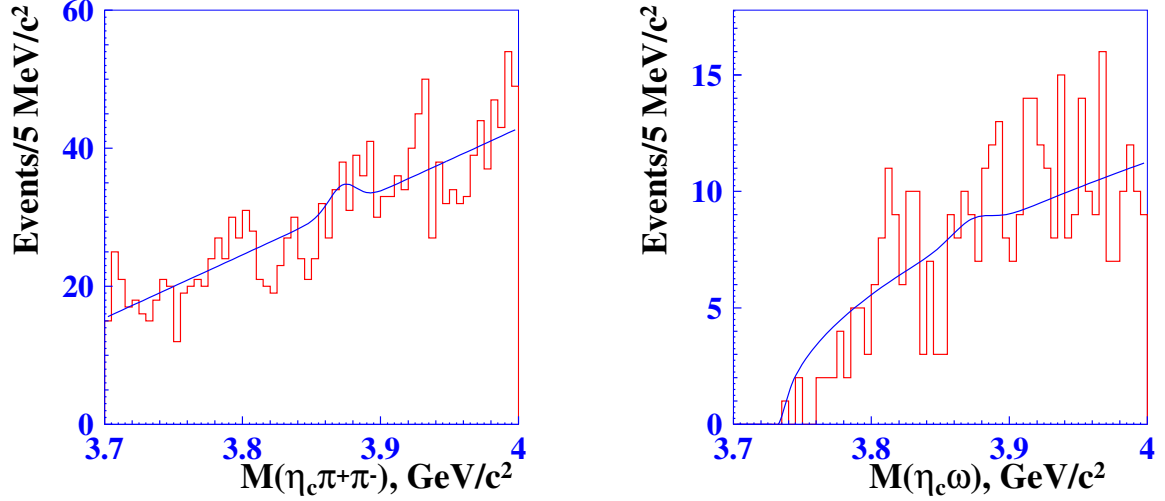


**Figure 5.** The distributions of  $\eta_c \pi^+ \pi^-$  (left) and  $\eta_c \omega$  (right) invariant masses in the search for the  $X_1(3872)$ . The threshold of the  $\eta_c \omega$  invariant mass is slightly shifted relative to the sum of the  $\omega$  and  $\eta_c$  nominal masses due to the mass windows of these two mesons, as confirmed by MC studies.

Decay mode	Fitting function	Efficiency, %	Yield
$X_1(3872) \rightarrow \eta_c \pi^+ \pi^-$	(3.6)	$7.95 \pm 0.02$	$17.9 \pm 16.5$
$X_1(3872) \rightarrow \eta_c \omega$	(3.7)	$1.92 \pm 0.02$	$6.0 \pm 12.5$
$X(3730) \rightarrow \eta_c \eta,$ $\eta \rightarrow \gamma\gamma$ $\eta \rightarrow \pi^+ \pi^- \pi^0$	(3.8)		
		$6.57 \pm 0.02$	$13.8 \pm 9.9$
		$1.18 \pm 0.01$	$1.4 \pm 1.0$
$X(3730) \rightarrow \eta_c \pi^0$	(3.10)	$6.52 \pm 0.02$	$-25.6 \pm 10.4$
$X(4014) \rightarrow \eta_c \eta,$ $\eta \rightarrow \gamma\gamma$ $\eta \rightarrow \pi^+ \pi^- \pi^0$	(3.9)		
		$7.09 \pm 0.02$	$8.9 \pm 11.0$
		$1.78 \pm 0.01$	$1.3 \pm 1.6$
$X(4014) \rightarrow \eta_c \pi^0$	(3.10)	$7.55 \pm 0.02$	$-8.1 \pm 13.2$

**Table 2.** Fit results for the  $X_1(3872)$ ,  $X(3730)$  and  $X(4014)$  resonances.

The  $\eta_c \eta$  invariant mass distributions in the  $X(4014)$  mass region are shown in figure 6 (bottom).

For the  $(\pi^0)$  mode, we use

$$f(x) = N_s G_{\text{LG}}(M, \sigma, P) + c_0 + c_1 x. \quad (3.10)$$

The  $\eta_c \pi^0$  invariant mass distributions are shown in figure 7.

The fit results are summarized in table 2.

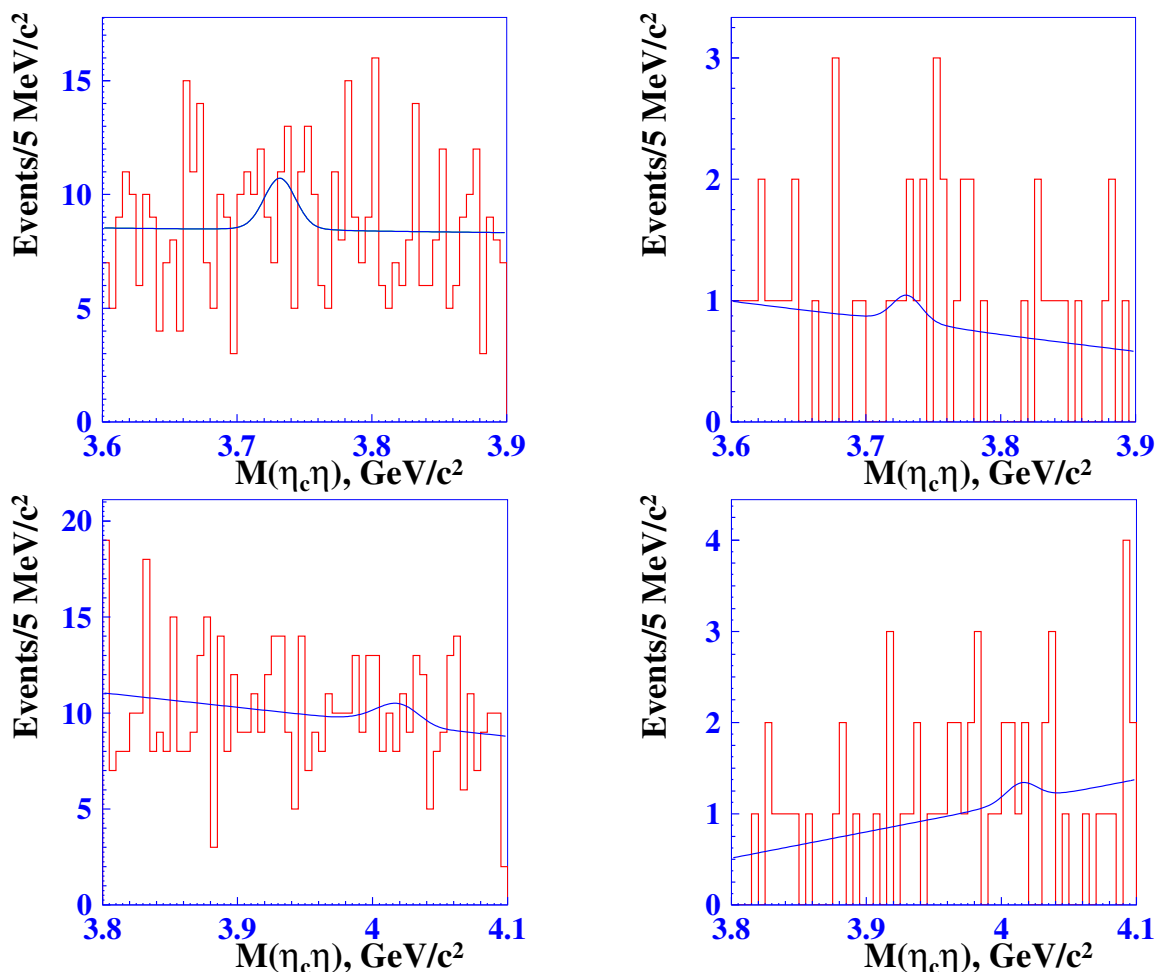


**Figure 6.** The combined fit projections of the  $\eta_c\eta$  invariant mass distributions in case of the  $\eta \rightarrow \gamma\gamma$  (left) and  $\eta \rightarrow \pi^+\pi^-\pi^0$  (right) modes corresponding to the search for the  $X(3730)$  (top) and  $X(4014)$  (bottom) resonances.

### 3.3 $Z(3900)^0$ and $Z(4020)^0$

We perform a sequence of binned maximum likelihood fits of the  $\eta_c\pi^+\pi^-$  invariant mass using the convolution of a Breit-Wigner and a Gaussian for the signal and a linear polynomial for the background:

$$f(x) = b(M, \Gamma) \otimes G(0, \sigma_{\text{res}}) + c_0 + c_1x. \quad (3.11)$$

The Gaussian models the detector resolution, which is assumed to be similar to that obtained in ref. [31] and equal to  $9.8 \text{ MeV}/c^2$ . The Breit-Wigner mass is confined to a  $20 \text{ MeV}/c^2$  window (the so-called mass bin) that is scanned in  $20 \text{ MeV}/c^2$  steps across the range  $(3.79\text{--}4.01) \text{ GeV}/c^2$  for the  $Z(3900)^0$  and  $(3.93\text{--}4.07) \text{ GeV}/c^2$  for the  $Z(4020)^0$ . The width is fixed to the weighted mean of the previously measured values ( $35 \text{ MeV}/c^2$  for the  $Z(3900)^0$  and  $12 \text{ MeV}/c^2$  for the  $Z(4020)^0$ ). The background is described by a linear polynomial. The detection efficiency is obtained from signal MC:  $(9.64 \pm 0.03)\%$  for the  $Z(3900)^0$  and  $(10.42 \pm 0.03)\%$  for the  $Z(4020)^0$ . The obtained signal yield is shown in

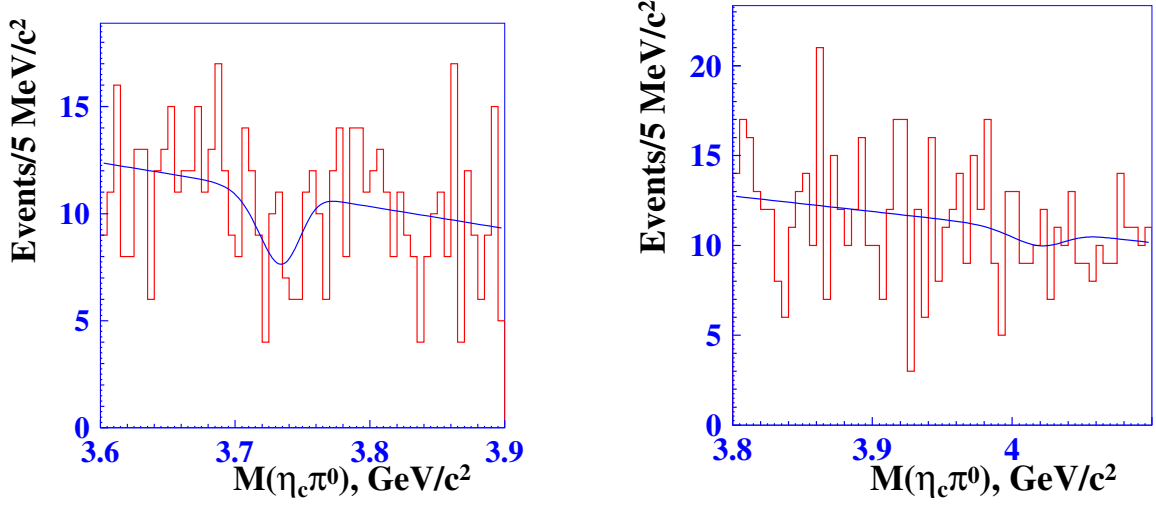


**Figure 7.** The  $\eta_c\pi^0$  invariant mass distributions corresponding to the search for the  $X(3730)$  (left) and  $X(4014)$  (right) resonances.

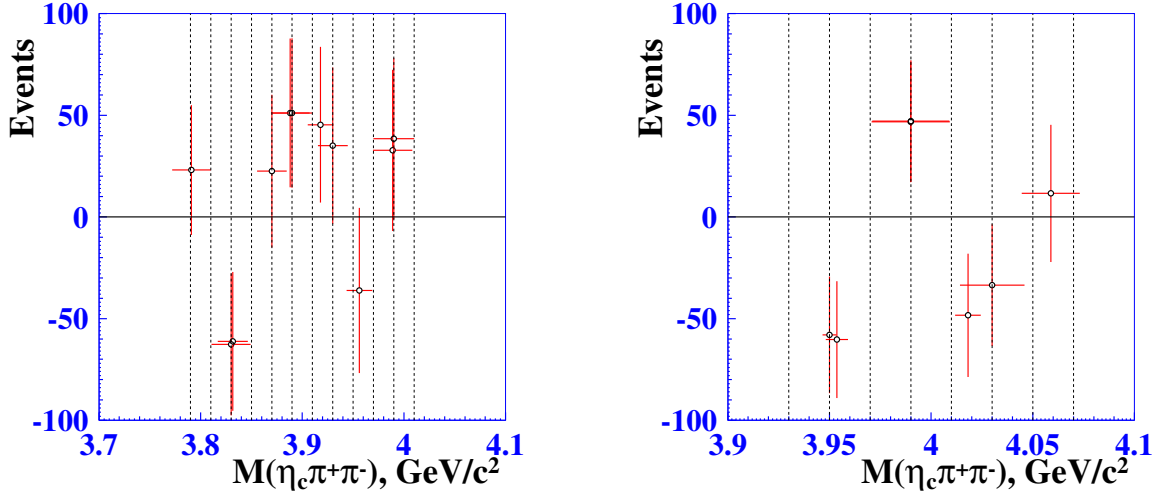


**Figure 8.** Dependence of the signal yield of the  $Z(3900)^0$  (left) and  $Z(4020)^0$  (right) on the mass bin. The mass bin is a  $20 \text{ MeV}/c^2$  window to which the mass is confined and scanned in  $20 \text{ MeV}/c^2$  steps across the fit range.

figure 8. The examples of the fit within the mass bin containing  $3.9 \text{ GeV}/c^2$  for  $Z(3900)^0$  and  $4.02 \text{ GeV}/c^2$  for  $Z(4020)^0$  are shown in figure 9.

### 3.4 $X(3915)$

For the  $\eta_c\eta$  invariant mass distribution, we perform a combined fit of two decay modes of the  $\eta$  meson:

$$f_i(x) = N_{\text{eff}}\varepsilon_i\mathcal{B}_i[b(M_i, \Gamma_i) \otimes G(0, \sigma_i)] + c_{0,i} + c_{1,i}x, \quad (3.12)$$

where  $N_{\text{eff}}$  is the effective number of signal events and  $i$  refers to either  $\eta \rightarrow \gamma\gamma$  or  $\eta \rightarrow \pi^+\pi^-\pi^0$  decay. The detector resolution  $\sigma_i$  is obtained from signal MC, taking into account

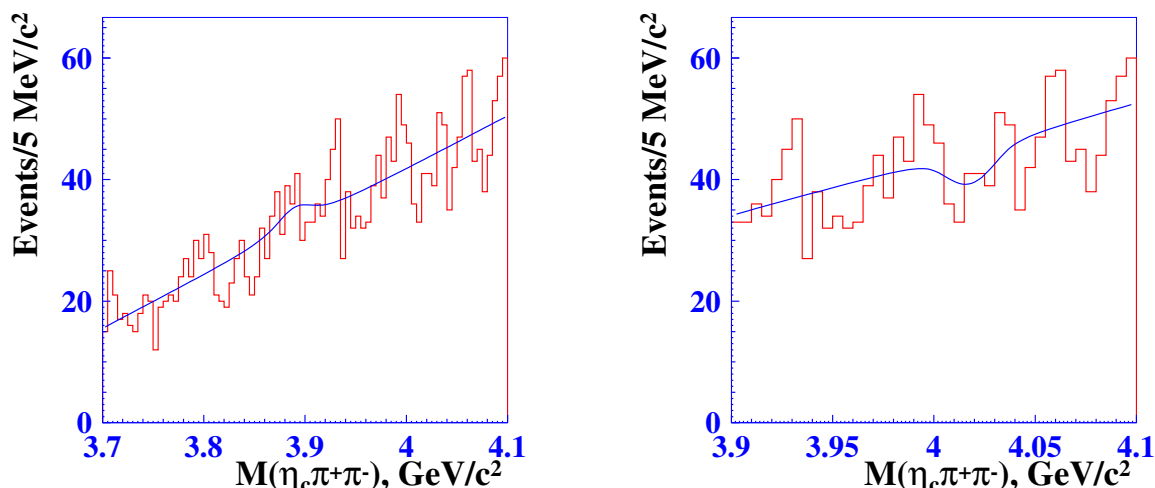


**Figure 9.** Examples of the fit within the mass bin containing  $3.9 \text{ GeV}/c^2$  for  $Z(3900)^0$  (left) and  $4.02 \text{ GeV}/c^2$  for  $Z(4020)^0$  (right).

the resolution degradation and is equal to  $13.6 \text{ MeV}/c^2$  for  $\eta \rightarrow \gamma\gamma$  and  $12.3 \text{ MeV}/c^2$  for  $\eta \rightarrow \pi^+\pi^-\pi^0$ . The corresponding  $\eta_c\eta$  invariant mass distribution is shown in figure 10.

We fit the  $\eta_c\pi^0$  invariant mass distribution with the function in eq. (3.11). The detector resolution is obtained from signal MC, taking into account the resolution degradation, and is equal to  $15.7 \text{ MeV}/c^2$ . The corresponding  $\eta_c\pi^0$  invariant mass distribution is shown in figure 11.

The fit results are summarized in table 3.

## 4 Systematic uncertainties

Systematic uncertainties are categorized as follows:

1. Additive systematic uncertainties affect the number of signal events and are estimated by the variation of the fit conditions. They are displayed as the numbers of events in tables 4 and 5 and arise from the sources listed below. (i) To obtain the error related to the resolution degradation, we vary the corrected variance of the fitting function within its statistical uncertainty. (ii) We assume that the combinatorial background can be parameterized with a first-order polynomial. To obtain the background shape uncertainty, we describe the background by a second-order polynomial and compare the results. For the ( $\omega$ ) mode, we change the square root to the fourth root. (iii) To estimate the systematic error associated with the selection criteria, we relax the criteria on  $\Delta E$ ,  $M_{bc}$ , and the invariant masses of  $\eta_c$ ,  $\omega$  and  $\eta$  by 50%. (iv) We vary the bin size between 2.5 to  $7.5 \text{ MeV}/c^2$  and determine the corresponding systematic error.
2. Multiplicative systematic uncertainties affect the product branching fractions. They are displayed in percent in table 6 and arise from the sources listed below. (i) The number of  $B\bar{B}$  pairs is calculated from the difference between the number of hadronic

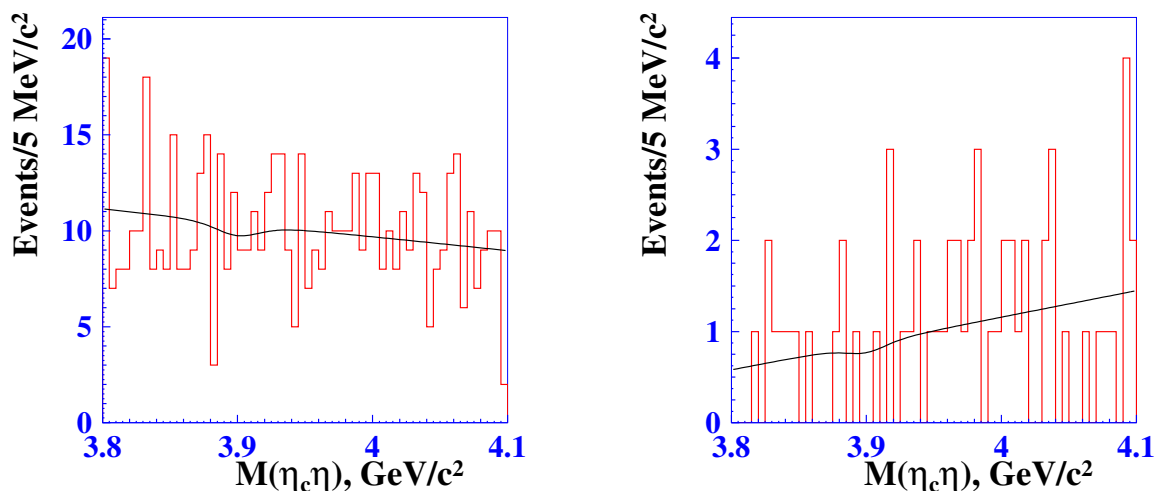


**Figure 10.** The combined fit projections of the  $\eta\eta$  invariant mass distributions in case of the  $\eta \rightarrow \gamma\gamma$  (left) and  $\eta \rightarrow \pi^+\pi^-\pi^0$  (right) modes corresponding to the search for the  $X(3915)$  resonance.

events on resonance and the scaled number of those off resonance. The systematic error is dominated by the uncertainty in the scale factor and is equal to  $\sim 1.4\%$  [32]. (ii) The uncertainties on the  $\omega$ ,  $\pi^0$ ,  $\eta$ ,  $\eta_c$  and  $K_S^0$  decay branching fractions are taken from ref. [33]. (iii) The statistical error of the efficiency determined by the signal MC is also taken as a systematic uncertainty. For  $Z(3900)^0$  and  $Z(4020)^0$  decays, we take into account the efficiency variation in the  $\eta_c\rho$  and  $\eta_cf_0$  decay modes. For the decays  $B^\pm \rightarrow K^\pm\eta_c\pi^+\pi^-$  and  $B^\pm \rightarrow K^\pm\eta_c\pi^0$ , we assume alternative decay modes containing intermediate  $K^{*0}$ ,  $K^*(1410)^\pm$  and  $\rho$  mesons, and take into account the difference of the MC detection efficiency as the corresponding systematic uncertainty. (iv) An analysis of the charged track reconstruction uncertainty as a function of particle momentum gives an estimate of 0.34% per charged track. (v) To determine the errors due to  $K$  and  $\pi$  meson identification, data from the analysis of the process  $D^{*+} \rightarrow D^0\pi^+$  followed by the decay  $D^0 \rightarrow K^-\pi^+$  are used. The uncertainty in  $K^\pm$  identification is 0.8% per  $K$  meson and the corresponding value for  $\pi^\pm$  identification is 0.5% per  $\pi$  meson. (vi) Estimation of the contribution of the  $\eta$  and  $\pi^0$  reconstruction uncertainty is carried out using the comparison of the number of reconstructed  $\eta \rightarrow 3\pi^0$  and  $\eta \rightarrow \gamma\gamma$  events. Such an estimate gives 2% per  $\eta$  and  $\pi^0$  meson. (vii) The contribution of the  $K_S^0$  reconstruction uncertainty is estimated to be 4.4% [34]. (viii) We also take into account the deviation of MC from the data by applying a correction to the efficiency:  $\varepsilon_{\text{Data}}/\varepsilon_{\text{MC}}$  is 0.9996 for each kaon and 0.9756 for each pion.

For the ( $\eta$ ) mode, the  $\eta$  meson is reconstructed in two decay modes:  $\eta \rightarrow \gamma\gamma$  and  $\eta \rightarrow \pi^+\pi^-\pi^0$ . To estimate the systematic uncertainty, we compare the systematic errors given by each  $\eta$  decay mode and take the maximum as the uncertainty for the reconstruction.

For the  $Z(3900)^0$  and  $Z(4020)^0$  decays to  $\eta_c\pi^+\pi^-$ , the additive systematic uncertainty is assumed to be the same as in  $X_1(3872) \rightarrow \eta_c\pi^+\pi^-$ . In addition, we vary the resonance width in the (15–65) MeV/ $c^2$  interval for the  $Z(3900)^0$  and (2.5–27.5) MeV/ $c^2$  interval

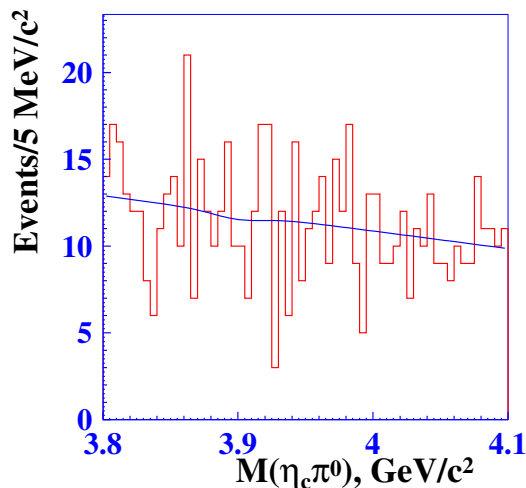


**Figure 11.** The  $\eta_c\pi^0$  invariant mass distribution corresponding to the search for the  $X(3915)$  resonance.

Decay mode	Fitting function	Efficiency, %	Yield
$X(3915) \rightarrow \eta_c\eta,$	(3.12)		
$\eta \rightarrow \gamma\gamma$		$6.60 \pm 0.02$	$-7.4 \pm 14.5$
$\eta \rightarrow \pi^+\pi^-\pi^0$		$1.64 \pm 0.01$	$-1.1 \pm 2.1$
$X(3915) \rightarrow \eta_c\pi^0$	(3.11)	$6.88 \pm 0.02$	$-4.3 \pm 18.1$

**Table 3.** Fit results for the  $X(3915)$  resonance.

Source	$\eta_c\pi^+\pi^-$	$\eta_c\omega$	$\eta_c\eta$	$\eta_c\pi^0$
Background parameterization	1	44	2687	2
Selection criteria	$< 1$	$< 1$	1695	33
Bin size	18	2	430	9
Total (events)	18	44	3206	34

**Table 4.** Additive systematic uncertainties (in events) for  $B$  decays without intermediate resonances. For the  $\eta_c\eta$  mode, the uncertainty corresponds to the effective number of events  $N_{\text{eff}}$ .

for the  $Z(4020)^0$ . The intervals are chosen according to the variation of the previously measured  $Z(3900)^\pm$  and  $Z(4020)^\pm$  width values. The total additive systematic uncertainty is 28.5 events for the  $Z(3900)^0$  and 25.9 events for the  $Z(4020)^0$ .

For the  $X(3915)$  decays, the systematic uncertainty is taken from the similar  $X(4014)$  decays (see tables 5 and 6).

## 5 Results

Our data sample does not permit us to measure the branching products of production and decay of the states listed above nor the  $B$  decay branching fractions so we set upper limits



Source	$\eta_c\pi^+\pi^-$	$\eta_c\omega$	$\eta_c\eta$		$\eta_c\pi^0$	
Mass, MeV/c <sup>2</sup>	3872	3872	3730	4014	3730	4014
Resolution degradation	1.2	< 1	68	28	1.4	0.2
Background parameterization	5.8	3.6	18	8	0.8	0.3
Selection criteria	23.9	5.4	293	280	5.2	9.3
Bin size	1.2	7.7	30	71	2.4	4.4
Total (events)	24.7	10.1	303	290	5.9	10.3

**Table 5.** Additive systematic uncertainties (in events) for  $B$  decays containing the  $X(3872)$ -like particles. For the  $\eta_c\eta$  mode, the uncertainty corresponds to the effective number of events  $N_{\text{eff}}$ .

Source	$\eta_c\pi^+\pi^-$	$\eta_c\omega$	$\eta_c\eta$	$\eta_c\pi^0$
Number of $B\bar{B}$ pairs	1.4	1.4	1.4	1.4
$\mathcal{B}(\omega \rightarrow \pi^+\pi^-\pi^0)$	—	0.8	—	—
$\mathcal{B}(\pi^0 \rightarrow \gamma\gamma)$	—	< 0.1	< 0.1	< 0.1
$\mathcal{B}(\eta \rightarrow \gamma\gamma)$	—	—	0.5	—
$\mathcal{B}(\eta \rightarrow \pi^+\pi^-\pi^0)$	—	—	1.2	—
$\mathcal{B}(\eta_c \rightarrow K_S^0 K^\pm \pi^\mp)$	6.8	6.8	6.8	6.8
$\mathcal{B}(K_S^0 \rightarrow \pi^+\pi^-)$	0.1	0.1	0.1	0.1
MC detection efficiency				
no resonance	35.8	2.4	1.3	19.5
$X(3872)$ -like	0.3	0.5	0.7	0.3
$Z(3900)^0/Z(4020)^0$	13.3/4.4	—	—	—
Track reconstruction	1.7	1.7	1.7	1.0
$K^\pm$ identification	1.6	1.6	1.6	1.6
$\pi^\pm$ identification	1.5	1.5	1.5	0.5
$\eta$ reconstruction	—	—	2.0	—
$\pi^0$ reconstruction	—	2.0	2.0	2.0
$K_S^0$ reconstruction	4.4	4.4	4.4	4.4
Total (%)				
no resonance	36.8	9.3	9.3	21.3
$X(3872)$ -like	8.7	9.0	9.2	8.7
$Z(3900)^0/Z(4020)^0$	15.9/9.7	—	—	—

**Table 6.** Multiplicative systematic uncertainties (in %).

instead, taking into account the statistical and systematic uncertainties. The expression for the required branching value is  $z = N_s/(N_B \varepsilon \mathcal{B}_i)$ , where  $N_s$  is the yield,  $N_B$  is the number

Decay mode	Upper limit (90% C.L.)
$B^\pm \rightarrow K^\pm \eta_c \pi^+ \pi^-$	$3.9 \times 10^{-4}$
$B^\pm \rightarrow K^\pm \eta_c \omega$	$5.3 \times 10^{-4}$
$B^\pm \rightarrow K^\pm \eta_c \eta,$	$2.2 \times 10^{-4}$
$B^\pm \rightarrow K^\pm \eta_c \pi^0$	$6.2 \times 10^{-5}$

**Table 7.** Results of branching fraction measurements for the  $B$  decays without an intermediate resonance.

Resonance	Decay mode	Upper limit (90% C.L.)
$X_1(3872)$	$\eta_c \pi^+ \pi^-$	$3.0 \times 10^{-5}$
	$\eta_c \omega$	$6.9 \times 10^{-5}$
$X(3730)$	$\eta_c \eta$	$4.6 \times 10^{-5}$
	$\eta_c \pi^0$	$5.7 \times 10^{-6}$
$X(4014)$	$\eta_c \eta$	$3.9 \times 10^{-5}$
	$\eta_c \pi^0$	$1.2 \times 10^{-5}$
$Z(3900)^0$	$\eta_c \pi^+ \pi^-$	$4.7 \times 10^{-5}$
$Z(4020)^0$		$1.6 \times 10^{-5}$
$X(3915)$	$\eta_c \eta$	$3.3 \times 10^{-5}$
	$\eta_c \pi^0$	$1.8 \times 10^{-5}$

**Table 8.** Results of branching fraction measurements for the  $B$  decays containing an intermediate exotic resonance. For  $Z(3900)^0$  and  $Z(4020)^0$  resonances the results are shown under the assumption that the masses are close to those of their charged partners.

of  $B\bar{B}$  pairs,  $\varepsilon$  is the detection efficiency, and  $\mathcal{B}_i$  is the product of the branching fractions of the intermediate resonances. This expression can be written as  $z = xy$ , where  $x = N_s$  and  $y = \frac{1}{N_{B\bar{B}}\varepsilon\mathcal{B}_i}$ . The distribution of the numerator  $N_s$  is assumed to be Gaussian with mean  $\mu$  and standard deviation  $\sigma_x = \sqrt{\sigma_{\text{stat}}^2 + \sigma_{\text{add. syst.}}^2}$ . The distribution of the inverse of the denominator is also assumed to be Gaussian with mean  $\nu = 1/(N_{B\bar{B}}\varepsilon\mathcal{B}_i)$  and standard deviation  $\sigma_y = \sigma_{\text{mult. syst.}}\nu$ . Thus, the distribution of  $z$  can be written in the following way:

$$F(z) = \int_{-\infty}^{+\infty} G(x, \mu, \sigma_x) G\left(\frac{z}{x}, \nu, \sigma_y \nu\right) \frac{1}{|x|} dx. \quad (5.1)$$

The 90% confidence level (C.L.) upper limit  $U$  on  $z$  is defined by

$$\frac{\int_0^U F(z) dz}{\int_0^\infty F(z) dz} = 0.9. \quad (5.2)$$

Upper limits on the branching fractions and products for all the studied decay modes are shown in tables 7 and 8.

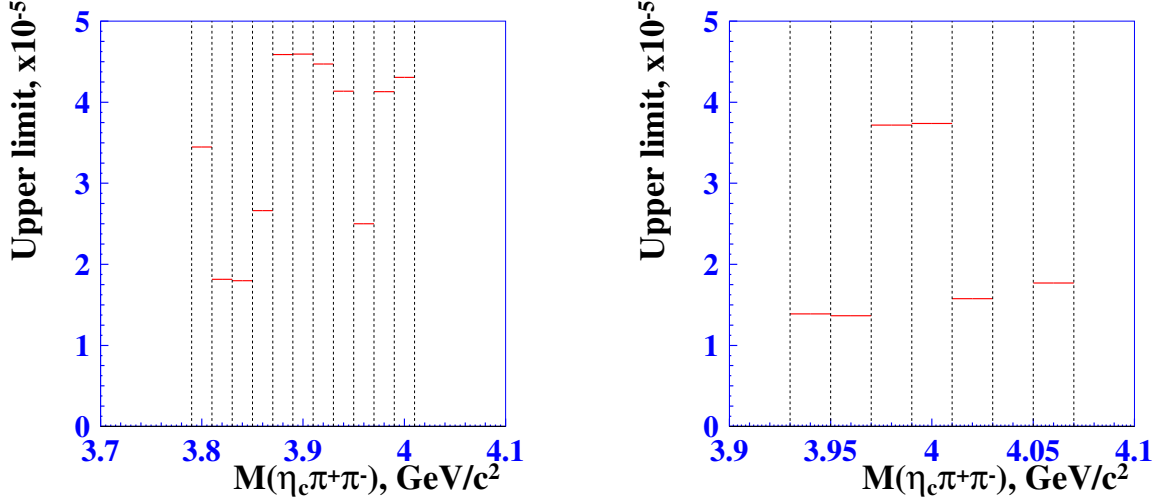


**Figure 12.** Dependence on the mass bin of the upper limit for the  $Z(3900)^0$  (left) and  $Z(4020)^0$  (right) branching product.

Figure 12 shows the dependence on the mass bin of the upper limit for the branching product of the  $Z(3900)^0$  and  $Z(4020)^0$  production and decay: no significant signal is seen in any of the invariant mass bins. For the  $Z(3900)^0$  resonance, we set upper limits in the range  $(1.8\text{--}4.7) \times 10^{-5}$  for the mass region  $(3.79\text{--}4.01) \text{ GeV}/c^2$ . For the  $Z(4020)^0$  resonance, we set upper limits in the range  $(1.6\text{--}3.7) \times 10^{-5}$  for the mass region  $(3.93\text{--}4.07) \text{ GeV}/c^2$ . If we assume that the  $Z(3900)^0$  and  $Z(4020)^0$  masses are close to those of their charged partners, we obtain the upper limits on the product branching fractions shown in table 8.

Similarly, for the study of  $X(3872)$ -like particles, we performed a mass scan inside the fitting region, i.e., a sequence of fits similar to the ones described above but with a mass floating in  $20 \text{ MeV}/c^2$ -wide mass bins. No significant signal is found in any of the studied bins.

A similar analysis was performed by BaBar [35], where the upper limit on the product  $\sigma(\gamma\gamma \rightarrow X(3872)) \times \mathcal{B}(X(3872) \rightarrow \eta_c \pi^+ \pi^-)$  was set.

In conclusion, we report a study of the following  $B$  decays to final states with  $\eta_c$ :  $B^\pm \rightarrow K^\pm \eta_c \pi^+ \pi^-$ ,  $B^\pm \rightarrow K^\pm \eta_c \omega$ ,  $B^\pm \rightarrow K^\pm \eta_c \eta$  and  $B^\pm \rightarrow K^\pm \eta_c \pi^0$ .

We first study these  $B$  decays without intermediate resonances and set 90% C.L. upper limits on their branching fractions:  $\mathcal{B}(B^\pm \rightarrow K^\pm \eta_c \pi^+ \pi^-) < 3.9 \times 10^{-4}$ ,  $\mathcal{B}(B^\pm \rightarrow K^\pm \eta_c \omega) < 5.3 \times 10^{-4}$ ,  $\mathcal{B}(B^\pm \rightarrow K^\pm \eta_c \eta) < 2.2 \times 10^{-4}$  and  $\mathcal{B}(B^\pm \rightarrow K^\pm \eta_c \pi^0) < 6.2 \times 10^{-5}$ .

We then assume that the decays proceed through intermediate molecular states similar to the exotic  $X(3872)$  particle, such as  $X_1(3872) = D^0 \bar{D}^{*0} - \bar{D}^0 D^{*0}$ ,  $X(3730) = D^0 \bar{D}^0 + \bar{D}^0 D^0$  and  $X(4014) = D^{*0} \bar{D}^{*0} + \bar{D}^{*0} D^{*0}$  and search for these states, setting 90% C.L. upper limits on the following product branching fractions:  $\mathcal{B}(B^\pm \rightarrow K^\pm X) \times \mathcal{B}(X \rightarrow \eta_c \pi^+ \pi^-) < 3.0 \times 10^{-5}$  and  $\mathcal{B}(B^\pm \rightarrow K^\pm X) \times \mathcal{B}(X \rightarrow \eta_c \omega) < 6.9 \times 10^{-5}$  for  $X = X_1(3872)$ ,  $\mathcal{B}(B^\pm \rightarrow K^\pm X) \times \mathcal{B}(X \rightarrow \eta_c \eta) < 4.6 \times 10^{-5}$  for  $X = X(3730)$  and  $< 3.9 \times 10^{-5}$  for  $X = X(4014)$ ,  $\mathcal{B}(B^\pm \rightarrow K^\pm X) \times \mathcal{B}(X \rightarrow \eta_c \pi^0) < 5.7 \times 10^{-6}$  for  $X = X(3730)$  and  $< 1.2 \times 10^{-5}$  for  $X = X(4014)$ .

We search for the neutral partners of the recently observed exotic states  $Z(3900)^\pm$  and  $Z(4020)^\pm$  and set 90% C.L. upper limits on the product branching fractions  $\mathcal{B}(B^\pm \rightarrow K^\pm Z) \times \mathcal{B}(Z \rightarrow \eta_c \pi^+ \pi^-)$  of  $4.7 \times 10^{-5}$  for  $Z = Z(3900)^0$  and  $1.6 \times 10^{-5}$  for  $Z = Z(4020)^0$ .

We set 90% C.L. upper limits on the following  $B$  decays involving the state  $X(3915)$ , whose origin is still unknown:  $\mathcal{B}(B^\pm \rightarrow K^\pm X(3915)) \times \mathcal{B}(X(3915) \rightarrow \eta_c \eta) < 3.3 \times 10^{-5}$  and  $\mathcal{B}(B^\pm \rightarrow K^\pm X(3915)) \times \mathcal{B}(X(3915) \rightarrow \eta_c \pi^0) < 1.8 \times 10^{-6}$ .

There are no theoretical predictions for the decay branching fractions of  $D^0 \bar{D}^{*0}$  molecular states similar to  $X(3872)$ . In this paper, we obtain an upper limit on the product branching fraction  $\mathcal{B}(B^\pm \rightarrow K^\pm X_1(3872)) \times \mathcal{B}(X_1(3872) \rightarrow \eta_c \pi^+ \pi^-)$ , which is of the same order as the product branching fraction  $\mathcal{B}(B^\pm \rightarrow K^\pm X(3872)) \times \mathcal{B}(X(3872) \rightarrow J/\psi \pi^+ \pi^-)$  measured in ref. [36]. A similar situation is observed with the upper limit on the  $\mathcal{B}(B^\pm \rightarrow K^\pm X(3915)) \times \mathcal{B}(X(3915) \rightarrow \eta_c \omega)$  and the value of  $\mathcal{B}(B^\pm \rightarrow K^\pm X(3915)) \times \mathcal{B}(X(3915) \rightarrow J/\psi \omega)$  obtained in ref. [19]. A more copious data set expected from the upcoming Belle II experiment [37] can provide an opportunity to determine the ratios of the decay branching fractions of the exotic states described above.

## Acknowledgments

We thank the KEKB group for the excellent operation of the accelerator; the KEK cryogenics group for the efficient operation of the solenoid; and the KEK computer group, the National Institute of Informatics, and the PNNL/EMSL computing group for valuable computing and SINET4 network support. We acknowledge support from the Ministry of Education, Culture, Sports, Science, and Technology (MEXT) of Japan, the Japan Society for the Promotion of Science (JSPS), and the Tau-Lepton Physics Research Center of Nagoya University; the Australian Research Council and the Australian Department of Industry, Innovation, Science and Research; Austrian Science Fund under Grant No. P 22742-N16 and P 26794-N20; the National Natural Science Foundation of China under Contracts No. 10575109, No. 10775142, No. 10875115, No. 11175187, and No. 11475187; the Ministry of Education, Youth and Sports of the Czech Republic under Contract No. LG14034; the Carl Zeiss Foundation, the Deutsche Forschungsgemeinschaft and the VolkswagenStiftung; the Department of Science and Technology of India; the Istituto Nazionale di Fisica Nucleare of Italy; National Research Foundation (NRF) of Korea Grants No. 2011-0029457, No. 2012-0008143, No. 2012R1A1A2008330, No. 2013R1A1A3007772, No. 2014R1A2A2A01005286, No. 2014R1A2A2A01002734, No. 2014R1A1A2006456; the Basic Research Lab program under NRF Grant No. KRF-2011-0020333, No. KRF-2011-0021196, Center for Korean J-PARC Users, No. NRF-2013K1A3A7A06056592; the Brain Korea 21-Plus program and the Global Science Experimental Data Hub Center of the Korea Institute of Science and Technology Information; the Polish Ministry of Science and Higher Education and the National Science Center; the Ministry of Education and Science of the Russian Federation and the Russian Federal Agency for Atomic Energy; the Slovenian Research Agency; the Basque Foundation for Science (IKERBASQUE) and the Euskal Herriko Unibertsitatea (UPV/EHU) under program UFI 11/55 (Spain); the Swiss National Science Foundation; the National Science Council and the Ministry of Education

of Taiwan; and the U.S. Department of Energy and the National Science Foundation. This work is supported by a Grant-in-Aid from MEXT for Science Research in a Priority Area (“New Development of Flavor Physics”) and from JSPS for Creative Scientific Research (“Evolution of Tau-lepton Physics”).

**Open Access.** This article is distributed under the terms of the Creative Commons Attribution License ([CC-BY 4.0](https://creativecommons.org/licenses/by/4.0/)), which permits any use, distribution and reproduction in any medium, provided the original author(s) and source are credited.

## References

- [1] BELLE collaboration, S.-K. Choi et al., *Observation of a narrow charmonium-like state in exclusive  $B^\pm \rightarrow K^\pm \pi^+ \pi^- J/\psi$  decays*, *Phys. Rev. Lett.* **91** (2003) 262001 [[hep-ex/0309032](#)] [[INSPIRE](#)].
- [2] CDF collaboration, D. Acosta et al., *Observation of the narrow state  $X(3872) \rightarrow J/\psi \pi^+ \pi^-$  in  $p\bar{p}$  collisions at  $\sqrt{s} = 1.96$  TeV*, *Phys. Rev. Lett.* **93** (2004) 072001 [[hep-ex/0312021](#)] [[INSPIRE](#)].
- [3] D0 collaboration, V.M. Abazov et al., *Observation and properties of the  $X(3872)$  decaying to  $J/\psi \pi^+ \pi^-$  in  $p\bar{p}$  collisions at  $\sqrt{s} = 1.96$  TeV*, *Phys. Rev. Lett.* **93** (2004) 162002 [[hep-ex/0405004](#)] [[INSPIRE](#)].
- [4] BABAR collaboration, B. Aubert et al., *Study of the  $B \rightarrow J/\psi K^- \pi^+ \pi^-$  decay and measurement of the  $B \rightarrow X(3872) K^-$  branching fraction*, *Phys. Rev. D* **71** (2005) 071103 [[hep-ex/0406022](#)] [[INSPIRE](#)].
- [5] LHCb collaboration, *Observation of  $X(3872)$  production in  $pp$  collisions at  $\sqrt{s} = 7$  TeV*, *Eur. Phys. J. C* **72** (2012) 1972 [[arXiv:1112.5310](#)] [[INSPIRE](#)].
- [6] LHCb collaboration, *Determination of the  $X(3872)$  meson quantum numbers*, *Phys. Rev. Lett.* **110** (2013) 222001 [[arXiv:1302.6269](#)] [[INSPIRE](#)].
- [7] M. Suzuki, *The  $X(3872)$  boson: Molecule or charmonium*, *Phys. Rev. D* **72** (2005) 114013 [[hep-ph/0508258](#)] [[INSPIRE](#)].
- [8] BABAR collaboration, B. Aubert et al., *Evidence for  $X(3872) \rightarrow \psi_{2S} \gamma$  in  $B^\pm \rightarrow X_{3872} K^\pm$  decays and a study of  $B \rightarrow c\bar{c} \gamma K$* , *Phys. Rev. Lett.* **102** (2009) 132001 [[arXiv:0809.0042](#)] [[INSPIRE](#)].
- [9] BELLE collaboration, V. Bhardwaj et al., *Observation of  $X(3872) \rightarrow J/\psi \gamma$  and search for  $X(3872) \rightarrow \psi' \gamma$  in  $B$  decays*, *Phys. Rev. Lett.* **107** (2011) 091803 [[arXiv:1105.0177](#)] [[INSPIRE](#)].
- [10] BELLE collaboration, Z.Q. Liu et al., *Study of  $e^+ e^- \rightarrow \pi^+ \pi^- J/\psi$  and Observation of a Charged Charmoniumlike State at Belle*, *Phys. Rev. Lett.* **110** (2013) 252002 [[arXiv:1304.0121](#)] [[INSPIRE](#)].
- [11] BESIII collaboration, M. Ablikim et al., *Observation of a Charged Charmoniumlike Structure in  $e^+ e^- \rightarrow \pi^+ \pi^- J/\psi$  at  $\sqrt{s} = 4.26$  GeV*, *Phys. Rev. Lett.* **110** (2013) 252001 [[arXiv:1303.5949](#)] [[INSPIRE](#)].
- [12] BESIII collaboration, M. Ablikim et al., *Observation of a charged  $(D\bar{D}^*)^\pm$  mass peak in  $e^+ e^- \rightarrow \pi D\bar{D}^*$  at  $\sqrt{s} = 4.26$  GeV*, *Phys. Rev. Lett.* **112** (2014) 022001 [[arXiv:1310.1163](#)] [[INSPIRE](#)].

- [13] T. Xiao, S. Dobbs, A. Tomaradze and K.K. Seth, *Observation of the Charged Hadron  $Z_c^\pm(3900)$  and Evidence for the Neutral  $Z_c^0(3900)$  in  $e^+e^- \rightarrow \pi\pi J/\psi$  at  $\sqrt{s} = 4170$  MeV*, *Phys. Lett. B* **727** (2013) 366 [[arXiv:1304.3036](#)] [[INSPIRE](#)].
- [14] BESIII collaboration, M. Ablikim et al., *Observation of a Charged Charmoniumlike Structure  $Z_c(4020)$  and Search for the  $Z_c(3900)$  in  $e^+e^- \rightarrow \pi^+\pi^-h_c$* , *Phys. Rev. Lett.* **111** (2013) 242001 [[arXiv:1309.1896](#)] [[INSPIRE](#)].
- [15] BESIII collaboration, M. Ablikim et al., *Observation of a charged charmoniumlike structure in  $e^+e^- \rightarrow (D^*\bar{D}^*)^\pm\pi^\mp$  at  $\sqrt{s} = 4.26$  GeV*, *Phys. Rev. Lett.* **112** (2014) 132001 [[arXiv:1308.2760](#)] [[INSPIRE](#)].
- [16] BELLE collaboration, K. Abe et al., *Observation of a near-threshold  $\omega J/\psi$  mass enhancement in exclusive  $B \rightarrow K\omega J/\psi$  decays*, *Phys. Rev. Lett.* **94** (2005) 182002 [[hep-ex/0408126](#)] [[INSPIRE](#)].
- [17] BABAR collaboration, B. Aubert et al., *Observation of  $Y(3940) \rightarrow J/\psi\omega$  in  $B \rightarrow J/\psi\omega K$  at BABAR*, *Phys. Rev. Lett.* **101** (2008) 082001 [[arXiv:0711.2047](#)] [[INSPIRE](#)].
- [18] BELLE collaboration, S. Uehara et al., *Observation of a charmonium-like enhancement in the  $\gamma\gamma \rightarrow \omega J/\psi$  process*, *Phys. Rev. Lett.* **104** (2010) 092001 [[arXiv:0912.4451](#)] [[INSPIRE](#)].
- [19] BABAR collaboration, P. del Amo Sanchez et al., *Evidence for the decay  $X(3872) \rightarrow J/\psi\omega$* , *Phys. Rev. D* **82** (2010) 011101 [[arXiv:1005.5190](#)] [[INSPIRE](#)].
- [20] BABAR collaboration, J.P. Lees et al., *Study of  $X(3915) \rightarrow J/\psi\omega$  in two-photon collisions*, *Phys. Rev. D* **86** (2012) 072002 [[arXiv:1207.2651](#)] [[INSPIRE](#)].
- [21] T. Branz, T. Gutsche and V.E. Lyubovitskij, *Hadronic molecule structure of the  $Y(3940)$  and  $Y(4140)$* , *Phys. Rev. D* **80** (2009) 054019 [[arXiv:0903.5424](#)] [[INSPIRE](#)].
- [22] X. Liu, Z.-G. Luo, Y.-R. Liu and S.-L. Zhu,  *$X(3872)$  and Other Possible Heavy Molecular States*, *Eur. Phys. J. C* **61** (2009) 411 [[arXiv:0808.0073](#)] [[INSPIRE](#)].
- [23] W.H. Liang, R. Molina and E. Oset, *Radiative open charm decay of the  $Y(3940)$ ,  $Z(3930)$ ,  $X(4160)$  resonances*, *Eur. Phys. J. A* **44** (2010) 479 [[arXiv:0912.4359](#)] [[INSPIRE](#)].
- [24] X. Liu, Z.-G. Luo and Z.-F. Sun,  *$X(3915)$  and  $X(4350)$  as new members in  $P$ -wave charmonium family*, *Phys. Rev. Lett.* **104** (2010) 122001 [[arXiv:0911.3694](#)] [[INSPIRE](#)].
- [25] S.L. Olsen, *Is the  $X(3915)$  the  $\chi_{c0}(2P)$ ?*, *Phys. Rev. D* **91** (2015) 057501 [[arXiv:1410.6534](#)] [[INSPIRE](#)].
- [26] S. Kurokawa and E. Kikutani, *Overview of the KEKB accelerators*, *Nucl. Instrum. Meth. A* **499** (2003) 1 [[INSPIRE](#)].
- [27] T. Abe et al., *Achievements of KEKB*, in *KEKB accelerator*, *Prog. Theor. Exp. Phys.* **2013** (2013) 03A001 [[INSPIRE](#)].
- [28] A. Abashian et al., *The Belle Detector*, *Nucl. Instrum. Meth. A* **479** (2002) 117 [[INSPIRE](#)].
- [29] BELLE collaboration, J. Brodzicka et al., *Physics achievements from the Belle experiment*, *Prog. Theor. Exp. Phys.* **2012** (2012) 04D001 [[arXiv:1212.5342](#)] [[INSPIRE](#)].
- [30] R. Brun, F. Carminati and S. Giani, *GEANT Detector Description and Simulation Tool*, CERN-W5013 (1994) [CERN-W-5013] [[INSPIRE](#)].
- [31] BELLE collaboration, A. Vinokurova et al., *Study of  $B^\pm \rightarrow K^\pm(K_S K \pi)^0$  Decay and Determination of  $\eta_c$  and  $\eta_c(2S)$  Parameters*, *Phys. Lett. B* **706** (2011) 139 [[arXiv:1105.0978](#)] [[INSPIRE](#)].

- [32] BELLE collaboration, K. Abe et al., *Measurement of branching fractions for  $B \rightarrow \pi\pi$ ,  $K\pi$  and  $KK$  decays*, *Phys. Rev. Lett.* **87** (2001) 101801 [[hep-ex/0104030](#)] [[INSPIRE](#)].
- [33] PARTICLE DATA GROUP collaboration, K.A. Olive et al., *Review of Particle Physics*, *Chin. Phys. C* **38** (2014) 090001 [[INSPIRE](#)].
- [34] BELLE collaboration, W.T. Chen et al., *A Study of  $\gamma\gamma \rightarrow K_S^0 K_S^0$  production at energies of 2.4 GeV to 4.0 GeV at Belle*, *Phys. Lett. B* **651** (2007) 15 [[hep-ex/0609042](#)] [[INSPIRE](#)].
- [35] BABAR collaboration, J.P. Lees et al., *Search for resonances decaying to  $\eta_c \pi^+ \pi^-$  in two-photon interactions*, *Phys. Rev. D* **86** (2012) 092005 [[arXiv:1206.2008](#)] [[INSPIRE](#)].
- [36] S.-K. Choi, S.L. Olsen, K. Trabelsi, I. Adachi, H. Aihara et al., *Bounds on the width, mass difference and other properties of  $X(3872) \rightarrow \pi^+ \pi^- J/\psi$  decays*, *Phys. Rev. D* **84** (2011) 052004 [[arXiv:1107.0163](#)] [[INSPIRE](#)].
- [37] BELLE-II collaboration, T. Abe et al., *Belle II Technical Design Report*, [arXiv:1011.0352](#) [[INSPIRE](#)].